

Ground Water Quality

Fracture-Controlled Nitrate and Atrazine Transport in Four Iowa Till Units

Martin F. Helmke,* William W. Simpkins, and Robert Horton

ABSTRACT

Fractures in till may provide pathways for agricultural chemicals to contaminate aquifers and surface waters. This study was conducted to quantify the influence of fractures on solute fate and transport using three conservative and two nonconservative tracers. The conservative tracers were potassium bromide (KBr), pentafluorobenzoic acid (PFBA), and 1,4-piperazinediethanesulfonic acid disodium salt (PIPES); the nonconservative tracers were nitrate and atrazine [6-chloro-*N*-ethyl-*N'*-(1-methylethyl)-1,3,5-triazine-2,4-diamine]. Three sites in Iowa were investigated, including four late Wisconsinan and Pre-Illinoian tills. Laboratory tracer experiments were conducted using eight large (0.4–0.45 m long by 0.43 m in diameter), undisturbed columns of till collected from depths of 1 to 28 m. The tills were densely fractured, with fracture spacing ranging from 3.8 to 10.4 cm. First arrival velocities of Br⁻ ranged from 0.004 to 64.8 m d⁻¹, 10 to 100 times faster than predicted for unfractured media. Nitrate behaved as a conservative tracer in weathered till columns, but degraded during experiments using deeper tills. Sorption caused retardation of atrazine in the shallowest four columns. Atrazine degradation occurred in deeper columns as demonstrated by deviations between atrazine and the conservative tracers. Mobile-immobile model (MIM) simulations estimated first-order exchange coefficients (α) ranging from 1×10^{-8} to $1.7 \times 10^{-2} \text{ s}^{-1}$, sorption coefficients (K_d) for atrazine ranging from 2.6×10^{-5} to $1 \times 10^{-3} \text{ m}^3 \text{ kg}^{-1}$, and degradation half-lives ranging from 0.24 to 67 d (nitrate) and 1.6 to 277 d (atrazine). This study suggests that aquifers and surface waters associated with thin, fractured till units may be vulnerable to contamination, yet deeper aquifers may be protected by these materials due to increased residence times provided by matrix diffusion.

TILL UNITS of Pre-Illinoian to late Wisconsinan age have generally been viewed as impermeable materials that preclude vertical and horizontal transport of surficial contaminants to aquifers and surface waters in Iowa. This idea has been extended to point sources such as landfills and hazardous waste sites and nonpoint sources including surface-applied nutrients and herbicides, and seepage of effluent from sewage and swine manure lagoons (Simpkins et al., 2002). Studies have suggested, however, that significant nitrate and herbicide contamination of the underlying aquifers has occurred in many areas. Samples of ground water from 686 rural wells in Iowa revealed that 35% of the state's shallow ground water was contaminated by NO₃-N above

the USEPA maximum contaminant level (MCL) of 10 mg L⁻¹ NO₃-N, and 18% contained detectable concentrations of herbicides (Kross et al., 1990). This may be an underestimate for herbicides, because detections are generally underreported when degradates are ignored (Kolpin et al., 2000). Aquifers confined by thinner till units (<15 m) show significantly more nitrate (35.1 vs. 12.8%) and pesticide (17.9 vs. 11.9%) detections than those confined by thicker (>15 m) till units (Kross et al., 1990). Contamination of aquifers by nonpoint sources migrating through the overlying till has been documented in Canada (McKay and Fredericia, 1995) and Denmark (Jørgensen and Fredericia, 1992; Jørgensen and Spliid, 1992). Evidence of contaminant plumes migrating down-gradient of landfills suggests that contaminants may also be transported laterally in till (D'Astous et al., 1989; Herzog et al., 1989; McKay et al., 1998).

Fractures or zones of preferential flow in till have been reported in Iowa (Kemmis et al., 1992) and elsewhere (Connell, 1984; Simpkins and Bradbury, 1992; Brockman and Szabo, 2000; Helmke, 2003), Canada (Keller et al., 1988; McKay et al., 1993a), and Denmark (Klint and Gravensen, 1999). Fractures promote greater velocities than would otherwise be expected under porous media assumptions (Freeze and Cherry, 1979; Grisak and Picken, 1980; Jørgensen and Spliid, 1992; McKay et al., 1993a, 1993b). A velocity increase occurs because the fractures increase the bulk hydraulic conductivity (K_b) of the till and reduce the effective porosity (θ_e). The K_b of a fractured till is typically one to three orders of magnitude greater than K_b for an unfractured till (Freeze and Cherry, 1979; Keller et al., 1989), while fracture porosity (θ_f) may be one to four orders of magnitude less than the total porosity (θ_T) of till (McKay et al., 1993a; Jørgensen et al., 1998). Advective velocity of solutes in fractured systems may be estimated by the average linear velocity equation:

$$V = K_b i / \theta_f \quad [1]$$

where V is velocity (m s⁻¹) and i is the hydraulic gradient (m m⁻¹). Fluid velocities up to 200 m d⁻¹ have been calculated for fractured till using Eq. [1] (Jørgensen et al., 1998). Typically, however, the processes of matrix diffusion, sorption, and degradation retard contami-

M.F. Helmke, Department of Geology, Dickinson College, Carlisle, PA 17013. W.W. Simpkins, Department of Geological and Atmospheric Sciences, Iowa State University, Ames, IA 50011. R. Horton, Agronomy Department, Iowa State University, Ames, IA 50011. Received 12 June 2003. *Corresponding author (helmkem@dickinson.edu).

Published in J. Environ. Qual. 34:227–236 (2005).

© ASA, CSSA, SSSA

677 S. Segoe Rd., Madison, WI 53711 USA

Abbreviations: α , first-order exchange coefficient; θ_e , effective porosity; θ_f , fracture porosity; BTC, breakthrough curve; C_0 , influent tracer concentration; D_0 , aqueous diffusion coefficient; d_1 , modified index of agreement; DML, Des Moines Lobe; IES, Iowan Erosion Surface; KBr, potassium bromide; K_b , bulk hydraulic conductivity; K_d , equilibrium sorption coefficient; MIM, mobile-immobile model; PFBA, pentafluorobenzoic acid; PIPES, 1,4-piperazinediethanesulfonic acid disodium salt; PV, pore volume; SIDP, Southern Iowa Drift Plain.

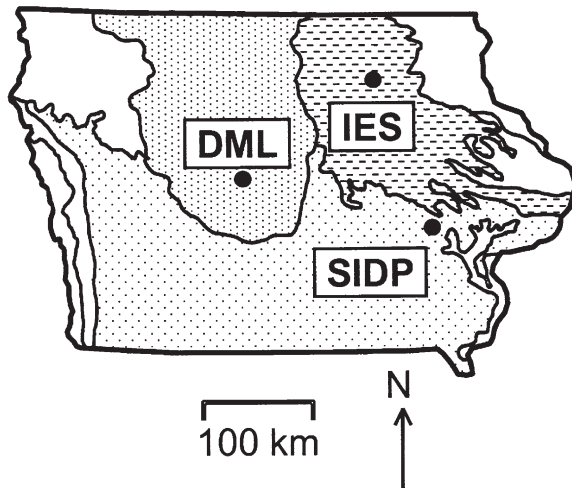


Fig. 1. Map showing the locations of the three study sites on the Des Moines Lobe (DML), Iowan Erosion Surface (IES), and Southern Iowa Drift Plain (SIDP) landform regions. Other mapped landform regions are given in Prior (1991).

nants as they pass through fractured till, allowing only a small percentage of a solute to travel at velocities calculated by Eq. [1] (Freeze and Cherry, 1979).

Research into the transport of nonpoint-source contaminants in till is lacking in areas of intensive agriculture (Rodvang and Simpkins, 2001). We hypothesize that transport of two common nonpoint-source contaminants found in ground water, nitrate and atrazine, is governed by fractures in the till and by diffusive exchange between the fractures and the till matrix. The purpose of this paper is to test this hypothesis using tracer experiments in large till columns. Results of the experiments will provide estimates of velocities and solute transport parameters useful for predicting transport of nonpoint-source contaminants in till.

MATERIALS AND METHODS

Site Descriptions

Three study sites set in areas of intensive agriculture and representing some of Iowa's youngest and oldest till units (ranging in age from 12 500 to >730 000 yr) in different landform regions were investigated (Fig. 1). Sites were also chosen because they allowed access to depths up to 30 m, and because previous studies had established the glacial stratigraphy and hydrogeology. The sites are herein referred to by their respective landform regions (Prior, 1991): the Des Moines Lobe site (DML), the Iowan Erosion Surface site (IES), and the Southern Iowa Drift Plain site (SIDP).

The DML site is located within the Walnut Creek watershed, 7 km south of Ames, IA. The Quaternary stratigraphy and hydrogeology of the Walnut Creek watershed was previously investigated as part of the Management Systems Evaluation Area (MSEA) program (Eidem et al., 1999). The surficial deposit at the DML site is the Alden Member till of the Dows Formation, deposited 14 000 to 12 500 yr ago during the late Wisconsinan (Prior, 1991; Eidem et al., 1999). The Alden Member is a massive, basal till with a bulk density of 1.70 Mg m^{-3} (Eidem et al., 1999). In the Des Moines Lobe, it averages 48% sand, 37% silt, and 15% clay and is classified as a loam to sandy loam (Kemmis et al., 1981). The Clarion

(fine-loamy, mixed, superactive, mesic Typic Hapludolls)–Nicollet (fine-loamy, mixed, superactive, mesic Aquic Hapludolls)–Webster (fine-loamy, mixed, superactive, mesic Typic Endoaquolls) soil association dominates the watershed and the soil series at the site is the Clarion silt loam.

The IES site is located 6 km southwest of Nashua, IA, on an agronomy research farm. Previous studies established the glacial stratigraphy and hydrogeology at the site (Weis and Simpkins, 1996). The material at the site includes a 1.1-m-thick section of late Wisconsinan to Holocene age pedis sediment above till of the Hickory Hills Member (Wolf Creek Formation), which is Pre-Illinoian in age (Kemmis et al., 1992). The upper half of the shallowest column was collected from the pedis sediment derived from till. The Hickory Hills till is a loam with 45% sand, 35% silt, and 20% clay and a bulk density ranging from 1.76 to 1.88 Mg m^{-3} (Kemmis et al., 1992). The Kenyon (fine-loamy, mixed, superactive, mesic Typic Hapludolls)–Floyd (fine-loamy, mixed, superactive, mesic Aquic Hapludolls)–Clyde (fine-loamy, mixed, superactive, mesic Typic Endoaquolls) soil association is present at the research farm and the soil series at the site is the Kenyon loam.

The SIDP site is near Coralville, IA, where a 30-m sequence of un lithified deposits had recently been removed for quarrying limestone. Stratigraphic studies at the site (Kemmis et al., 1992) reported the presence of till of the Hickory Hills, Aurora, and Winthrop Members of the Wolf Creek Formation (500 000–730 000 yr old), and till of the Alburnett Formation (>730 000 yr old). The till units are loams that contain 30 to 50% sand, 30 to 45% silt, and 20 to 25% clay. Bulk densities range from 1.76 to 2.11 Mg m^{-3} . The deepest and oldest till unit is part of the Alburnett Formation, which has a higher bulk density (1.97 to 2.11 Mg m^{-3} ; Kemmis et al., 1992). The Fayette (fine-silty, mixed, superactive, mesic Typic Hapludalfs)–Downs (fine-silty, mixed, superactive, mesic Mollic Hapludalfs) soil association occurs on uplands and the main soil series in the area is the Fayette silt loam.

Fracture Mapping and Column Preparation

Fractures were mapped at each site to document their occurrence and density. A backhoe was used to excavate soil pits at the DML and IES sites, which were 3.9 and 2.3 m deep, respectively. Active quarry operations at the SIDP site allowed convenient access to fresh till faces to a depth of about 30 m. The walls of the excavation pits were constructed using a bench and tier system, which increased the stability of the walls and provided multiple dihedral faces for mapping fractures and collecting samples. Till exposures were further prepared using a hand trowel and putty knife to ensure that exposed till was fresh and undisturbed by backhoe excavation. Fractures were identified by iron-stained halos or other evidence of leaching along fracture surfaces. Fractures from both horizontal and vertical faces were traced onto sheets of clear acetate and later digitized. Average fracture spacing ($2B$) was measured in the field along horizontal scan lines using a fiberglass tape.

Till was removed from benches in the soil pits using hand trowels and putty knives leaving free-standing columns of intact till, approximately 43 cm in diameter and 50 cm in length. The columns were collected from depths between 1.0 and 27.95 m (Table 1). Each column was kept in cylindrical form using a level and a section of polyvinyl chloride (PVC) pipe as guides. A 61-cm-long piece of flexible PVC with a 45.7-cm i.d. was placed over each column, leaving about a 1- to 1.5-cm void between the column and the pipe. In the field, the annulus between the till and the casing was sealed with paraffin wax to prevent sidewall flow (Grisak et al., 1980;

Table 1. Location, depth, stratigraphic classification, weathering status (WS), bulk density (ρ_b), total porosity (θ_T), texture, and bulk hydraulic conductivity (K_b) of the eight columns collected for this study.

Column†	Depth	Formation, member	WS‡	ρ_b	θ_T	Sand	Silt	Clay	K_b
	m			Mg m ⁻³		%			m s ⁻¹
DML-1	1.00–1.45	Dows, Alden	W	1.67	29.8	49.3	35.3	15.4	3.8×10^{-5}
DML-2	2.00–2.45	Dows, Alden	W	1.84	30.5	52.1	33.5	14.4	2.3×10^{-6}
DML-3	3.3–3.7	Dows, Alden	PW	1.83	29.6	50.7	34.5	14.8	6.8×10^{-8}
IES-1	1.25–1.70	Wolf Creek, Hickory Hills	W	1.82	31.2	41.2	31.3	27.5	7.1×10^{-6}
IES-2	1.50–1.90	Wolf Creek, Hickory Hills	W	1.86	30.7	46.6	30.7	22.7	2.8×10^{-6}
SIDP-1	10.50–10.95	Wolf Creek, Aurora	W	1.82	30.5	39.9	35.6	24.5	1.3×10^{-8}
SIDP-2	16.50–16.95	Wolf Creek, Aurora	PW	1.89	28.8	33.5	39.1	27.4	4.7×10^{-9}
SIDP-3	27.50–27.95	Alburnett, NA	U	2.01	28.6	33.5	43.1	23.4	7.7×10^{-10}

† DML, Des Moines Lobe; IES, Iowan Erosion Surface; SIDP, Southern Iowa Drift Plain. See Fig. 1 for locations.

‡ W, weathered; PW, partially weathered; U, unweathered.

Kluitenberg et al., 1991). After the wax cooled (approximately 8 h), a putty knife was used to separate the column from the in situ till base and the column was lifted from the excavation trench. Disks of high-density polyethylene (HDPE) with a thickness of 3 mm were placed at the column ends and sealed with wax to prevent moisture loss during transport to the laboratory.

In the laboratory, the column ends were carefully scraped and roughened with a putty knife to minimize smearing of the till. Ottawa sand was placed in 5-mm-thick layers at the column ends and held in place by the HDPE disks. Perforated HDPE tubes with a 3-mm i.d. were pressed into the sand to provide fluid access to the sand packs. Pistons consisting of 19-mm-thick plywood were added to the column ends and sealed with silicone caulking. The ends and the walls of the columns were mechanically compressed to a pressure approximately equal to in situ lithostatic conditions. A pressure of 60 kPa, equivalent to a depth of approximately 3.5 m, was the maximum pressure that could be obtained by this method. Although great care was exercised to minimize desaturation of the columns, it is possible that some of the larger pores drained during excavation and transport. Each column was slowly resaturated by upward flow for at least 7 d to reduce the chance of entrapped air within pores.

Ground water collected from each site was induced to flow through the columns under a constant upward gradient. A unit hydraulic gradient was applied to the DML-2, DML-3, IES-1, IES-2, SIDP-1, SIDP-2, and SIDP-3 columns. A gradient of 0.021 was applied to the DML-1 column (the most permeable column collected) to reduce the flow rate from 330 to 6.93 mL min⁻¹. Although an upward gradient was applied (to prevent desaturation at the column base), ground water flow was, in effect, downward because each column was inverted in the laboratory. Column temperature was maintained at a constant 12°C to simulate in situ conditions. Flow rates were monitored and K_b was calculated using the Darcy equation (Helmke, 2003).

Soil texture was determined using the sieve and pipette method (Walter et al., 1978). Sand, silt, and clay particle sizes used in this study were 2 to 0.05, 0.05 to 0.002, and <0.002 mm, respectively. Bulk density (ρ_b) was determined by collecting samples in cylinders of known volume and weighing them after being dried for 24 h at 104°C. Total porosity (θ_T) was determined gravimetrically by weighing saturated samples, oven-drying them, dividing the difference by the density of water, and dividing this by the original volume of each sample. Pore volume (PV) was calculated as the product of θ_T and the volume of each column.

Tracer Experiments

Five tracers were used in the experiments: potassium bromide (KBr), pentafluorobenzoic acid (PFBA), 1,4-piperazine-

diethanesulfonic acid disodium salt (PIPES), potassium nitrate (KNO₃), and atrazine. Nitrate (a nutrient) and atrazine (a broadleaf herbicide) were chosen as tracers because nitrate (applied as ammonia) and atrazine are agricultural chemicals frequently used in Iowa and are also found in ground water (Eidem et al., 1999; Moorman et al., 1999). Conservative compounds of differing aqueous diffusion coefficients (D_0) (Br⁻, PFBA, and PIPES) were selected because differences in the morphology of their breakthrough curves (BTCs) would indicate matrix diffusion and provide evidence of fracture flow and fracture–matrix interaction. The D_0 values of Br⁻, PFBA, PIPES, NO₃⁻, and atrazine are 1.8×10^{-9} , 7.6×10^{-10} , 4.1×10^{-10} , 1.6×10^{-9} , and 6.6×10^{-10} m² s⁻¹, respectively (National Research Council, 1929; Scott and Phillips, 1973; Bowman and Gibbens, 1992; Helmke et al., 2004). The use of conservative tracers with unique diffusion coefficients has been used to demonstrate matrix diffusion in soil with macropores (Mayes et al., 2003) and fractured saprolite (Moline et al., 1997), but has not previously been applied to studies of fractured till.

An influent tracer concentration (C_0) of 0.5 mM was used for KBr, PFBA, PIPES, and KNO₃, which is equivalent to 39.95 mg L⁻¹ Br⁻, 106.04 mg L⁻¹ PFBA, 167.69 mg L⁻¹ PIPES, and 31.5 mg L⁻¹ NO₃⁻, respectively. The concentration of NO₃⁻ was chosen because it is similar to the maximum contaminant level (MCL) of 45 mg L⁻¹ (as NO₃⁻). Molar concentrations of Br⁻, PFBA, and PIPES were then set to equal that of nitrate. The resulting concentration of PFBA was similar to that used in previous studies in Iowa (Jaynes, 1993). The C_0 of atrazine of 4.64 μ M (1 mg L⁻¹) was chosen to reduce the amount of waste atrazine produced, while still providing a sufficient concentration to ensure instrument detection.

The tracer solution was introduced to each column under a constant hydraulic gradient using a Mariotte bottle. The experiments for shallow columns DML-1, IES-1, IES-2, and DML-2 lasted 3.0 d (1.5 PV), 0.5 d (2.2 PV), 1.4 d (2.8 PV), and 2.0 d (2.9 PV), respectively. The tracer solution for DML-1, IES-1, IES-2, and DML-2 was applied for 1.0 d (0.51 PV), 0.167 d (0.73 PV), 0.47 d (0.93 PV), and 0.67 d (0.97 PV), respectively, and then rinsed with clean water until the end of each experiment. Experiments in the deeper columns (DML-3, SIDP-1, SIDP-2, and SIDP-3) lasted for 70 d (3.4 PV), 117 d (0.93 PV), 90 d (0.28 PV), and 145 d (0.075 PV), respectively, and were not rinsed due to time constraints.

Effluent samples were passed through a 0.2- μ m filter immediately on collection and stored at 4°C until analyzed at the end of each experiment. Bromide, PFBA, PIPES, and nitrate concentrations were determined by ion chromatography. Atrazine concentrations were analyzed by high performance liquid chromatography (HPLC) at the National Soil Tilth Laboratory in Ames, IA. Analytical precision for Br⁻ (± 0.63 mg L⁻¹), PFBA (± 1.14 mg L⁻¹), PIPES (± 2.65 mg L⁻¹), nitrate (± 0.10 mg L⁻¹), and atrazine (± 0.01 mg L⁻¹) was determined from replicates of spiked samples (Harris, 1991).

At the end of the tracer experiment, a 1 g L⁻¹ solution of FDC Brilliant Blue Dye no. 1 was introduced to the DML-3 column for one day under a hydraulic gradient of 3 (0.15 PV). The column was then dissected to determine if the dye followed the fractures. This dye is commonly used by soil scientists because its bright blue color is distinguishable from the brown color of most soils and it is nontoxic (Flury and Flühler, 1995). Upon drainage, the column was dissected into 5-cm horizontal slices. Both iron-stained fractures and the regions of blue-stained soil were mapped onto sheets of clear acetate and digitized.

Mobile-Immobile Model

Solute transport parameters were estimated from the column data using the mobile-immobile model (MIM). Its application to saturated flow in fractured till is new. However, the MIM approach has been widely used by soil physicists to simulate solute transport through soil containing macropores. It simulates a dual porosity medium as a region in which fluid is moving (the fractures) and a region where fluid is stagnant (the soil or till matrix). The model simulates exchange between the regions as a first-order process (Coats and Smith, 1964). The MIM does not require explicit knowledge of pore geometry (or fracture orientation in this case), which is an advantage when simulating a dense network of macropores near the soil surface. The model's computational efficiency also allows it to be used in the inverse mode (van Genuchten, 1981; Parker and van Genuchten, 1984; Gaber et al., 1995).

The MIM was developed by Coats and Smith (1964) and later modified to include solute sorption (van Genuchten and Wierenga, 1976) and degradation (van Genuchten and Wagenet, 1989). It includes governing equations for the mobile region (Eq. [2]) and immobile region (Eq. [3]) (van Genuchten and Wagenet, 1989):

$$(\theta_m + f\rho_b K_d) \frac{\partial c_m}{\partial t} = \theta_m D_m \frac{\partial^2 c_m}{\partial x^2} - J_w \frac{\partial c_m}{\partial x} - \alpha(c_m - c_{im}) - (\theta_m \mu + f\rho_b K_d \mu) c_m \quad [2]$$

$$[\theta_{im} + (1 - f)\rho_b K_d] \frac{\partial c_{im}}{\partial t} = \alpha(c_m - c_{im}) - [\theta_{im} \mu + (1 - f)\rho_b K_d \mu] c_{im} \quad [3]$$

where c_m and c_{im} are solute concentrations in the mobile and immobile regions (kg m⁻³), θ_m and θ_{im} are the mobile and immobile region porosities (m³ m⁻³), t is time (s), D_m is the dispersion coefficient for the mobile region (m² s⁻¹), x is distance along the flowpath (m), J_w is the volumetric flux (specific discharge, m s⁻¹), α is the first-order exchange coefficient (s⁻¹), K_d is the equilibrium-sorption coefficient (m³ kg⁻¹), f is the fraction of adsorption sites in the mobile region, and μ is the degradation coefficient (s⁻¹). A semi-analytical solution for Eq. [2] and [3] was developed by van Genuchten and Wagenet (1989). The computer program CXTFIT 2.1 (Toride et al., 1999) solves the equation in the inverse mode using a nonlinear method of least squares (Marquardt, 1963).

The MIM is not strictly a fracture-flow model, because it does not incorporate fracture geometry. However, by substituting θ_f for θ_m , the MIM can reproduce BTCs generated by discrete-fracture models (Sudicky, 1990). Assuming that fractures are equally spaced, vertical, and orthogonal plates, θ_m may be calculated by the equation (Sudicky, 1990):

$$\theta_m = 2 \frac{2b}{2B} \quad [4]$$

where $2b$ is fracture aperture (m) and $2B$ is average fracture spacing (m). Fracture aperture was estimated using the Cubic Law (Snow, 1969):

$$2b = \left(\frac{K_b 6\mu 2B}{\rho g} \right)^{\frac{1}{3}} \quad [5]$$

where μ is fluid viscosity (kg m⁻¹ s⁻¹), ρ is fluid density (kg m⁻³), and g is the acceleration due to gravity (m s⁻²). In this study, values of θ_m from field and laboratory measurements were used as input for the MIM.

Statistical Analysis

The goodness-of-fit between the observed tracer test data and data predicted by the MIM was evaluated using the modified index of agreement, d_1 (Willmott et al., 1985). The parameter d_1 is given by:

$$d_1 = 1.0 - \frac{\sum_{i=1}^N |O_i - P_i|}{\sum_{i=1}^N (|P_i - \bar{O}| + |O_i - \bar{O}|)} \quad [6]$$

where O and P are the observed and model-simulated data, respectively, \bar{O} is the mean of the observed values, and N is the number of observations. The value of d_1 varies from 0 to 1, with 1 indicating a perfect fit between the simulated and observed data. Therefore, the value of d_1 may be interpreted in a similar fashion as the coefficient of determination (R^2), although d_1 is considered superior to R^2 because d_1 is less sensitive to outliers and because it is more sensitive to additive and proportional differences than R^2 . The d_1 approach has been applied elsewhere to evaluate the goodness-of-fit of hydrologic models (Legates and McCabe, 1999).

RESULTS AND DISCUSSION

Physical Properties

Measurements of the physical properties of the columns indicate values consistent with previous studies (Table 1). Columns representing the Dows Formation contain the sandiest till, ranging from 49.3 to 52.1% sand. Less sand and greater clay percentages (up to 27.4%) were characteristic of columns from Pre-Illinoian till units. Bulk densities range from 1.67 Mg m⁻³ in weathered till of the Dows Formation to 2.01 Mg m⁻³ in unweathered till of the Alburnett Formation. Total porosities showed a small range of values, from 28.6% in the SIDP-3 column to 31.2% in the IES-1 core. Values of K_b were similar to those estimated from slug tests at these and nearby sites (Seo, 1996; Seo et al., 1996; Weis and Simpkins, 1996) and values generally decrease with depth.

Fracture Orientation and Density

Fractures were encountered at all three sites and at each of the depths evaluated, although the fracture patterns and the density of fractures differed. Fractures observed near the base of the DML excavation trench were dense, primarily subvertical, and oriented in a northeast-southwest pattern (Fig. 2a). The average fracture spacing at a depth of 3.3 m was 4.3 cm and the fracture density was 260 fractures m⁻². In contrast, fractures at the IES site lack a preferred orientation (Fig.

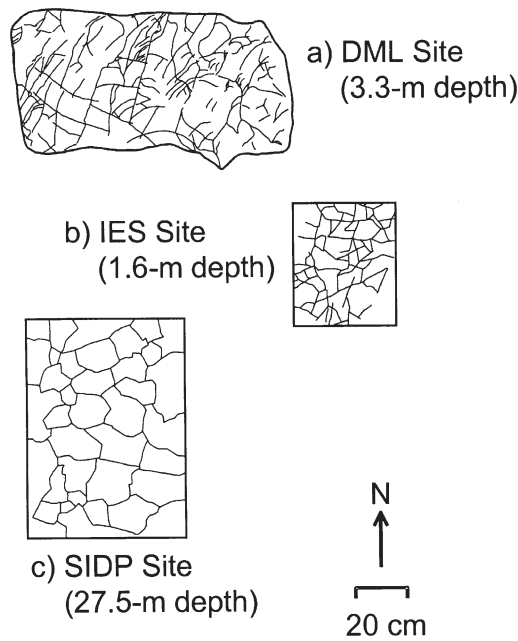
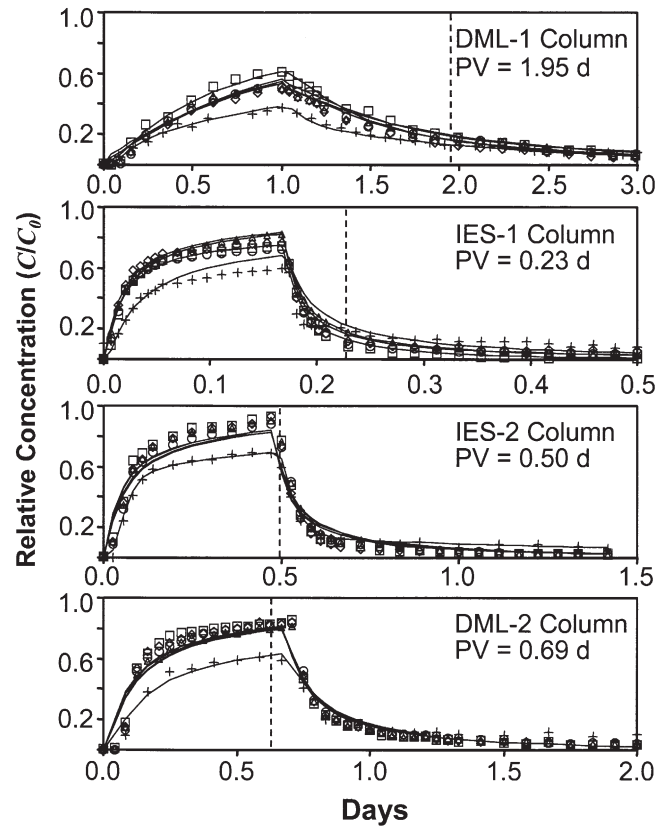


Fig. 2. Plan view maps of fracture patterns at the (a) Des Moines Lobe (DML) site, (b) Iowan Erosion Surface (IES) site, and (c) Southern Iowa Drift Plain (SIDP) site.

2b). The average fracture spacing at a depth of 1.6 m was 3.8 cm and fracture density was 145 fractures m^{-2} . Fractures at the SIDP site consisted of widely spaced, distinct polygons (Fig. 2c). At the sample depth of 27.5 m, average fracture spacing was 10.4 cm and fracture density was 221 fractures m^{-2} . The observed fracture spacing of less than 5 cm at shallow depths (<2 m) is consistent with studies in Canada (McKay et al., 1993a) and Denmark (Klint and Gravensen, 1999), although larger fracture spacings (>8 m) were reported at depths greater than 4 m by the Canadian and Danish studies. Given the dense fracture spacing observed in this study, each column was of adequate size to collect numerous fractures. However, it should be noted that the results from an individual column may not be representative of an entire till unit, as properties of fractures are likely to be variable spatially, and no replicate samples were collected in this study.

Tracer Experiments

Breakthrough curves produced during the laboratory experiments were consistent with solute transport controlled by macropores or fractures (Fig. 3 and 4). In the absence of such features and assuming no dispersion, breakthrough should have occurred after 1 PV had passed through each column. However, first arrival of the tracers occurred substantially before 1 PV in all eight experiments. Measurable concentrations of the conservative tracers (Br^- , PFBA, and PIPES) appeared in the column effluent ($C/C_0 > 0.02$; the instrument detection limit) within 0.1 PV. We define here a velocity of Br^- , or V_{Br} , corresponding to this time of first arrival. Observed V_{Br} ranged from 0.004 to 64.8 $m d^{-1}$, versus 0.0002 to 1.97 $m d^{-1}$ as calculated using the average linear velocity equation Eq. [7] (Fig. 5):



○ Br^- ◇ PFBA □ PIPES △ $NO_3 + Atrazine$ — MIM Fit

Fig. 3. Observed and modeled breakthrough curves generated from the DML-1, IES-1, IES-2, and DML-2 columns, where DML is the Des Moines Lobe and IES is the Iowan Erosion Surface. The dashed vertical line indicates the time for 1 pore volume (PV) to pass through each column. MIM, mobile-immobile model; PFBA, pentafluorobenzoic acid; PIPES, 1,4-piperazinediethanesulfonic acid disodium salt.

$$V_{PM} = K_{bi}/\theta_m \quad [7]$$

Similarly, the V_{Br} reported from a field-tracer test in fractured till in Ontario, Canada, was 0.05 $m d^{-1}$, nearly 10 times greater than the average V_{PM} of 0.006 $m d^{-1}$ (McKay et al., 1993b). Jørgensen et al. (1998) observed the first arrival velocity of chloride of 2.8 $m d^{-1}$ in a large till column under a unit hydraulic gradient; the calculated V_{PM} was only 0.2 $m d^{-1}$. Velocities (Fig. 5) were also not dependent on depth, fracture patterns, or age of the till (Fig. 2), which suggests that late Wisconsinan and Pre-Illinoian till units are equally susceptible to fracture flow.

Differences of BTC morphology among the conservative tracers (Br^- , PFBA, and PIPES) provide additional evidence of macropore- or fracture-controlled solute transport combined with diffusion into the till matrix. Matrix diffusion, the process whereby solutes are exchanged between the matrix (immobile region) and macropore or fracture (mobile region) due to a concentration gradient, effectively retards solutes as they pass through the column. If matrix diffusion is occurring, the rate at which solutes increase in concentration during the rising limbs of BTCs should be inversely proportional to the respec-

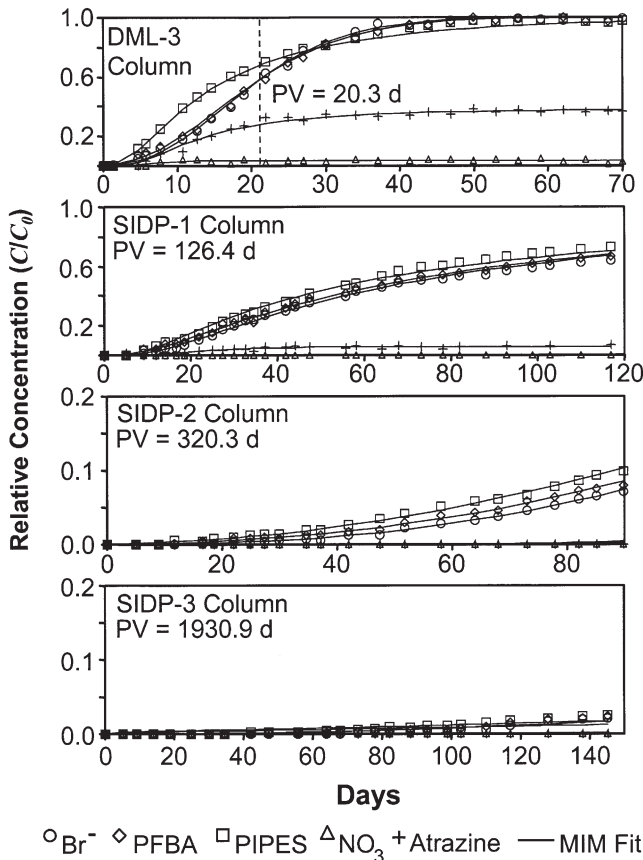


Fig. 4. Observed and modeled breakthrough curves generated from the DML-3, SIDP-1, SIDP-2, and SIDP-3 columns, where DML is the Des Moines Lobe and SIDP is the Southern Iowa Drift Plain. The dashed vertical line for the DML-3 column indicates the time for one pore volume (PV) to pass through the column. The pore volumes were off scale for the SIDP-1, SIDP-2, and SIDP-3 columns.

tive D_0 values (i.e., PIPES will increase in concentration first, followed by PFBA and then Br^-). There should be a similar separation of the solute concentrations during the falling limbs, or tails, of the BTCs (Moline et al., 1997; Gwo et al., 1998). This phenomenon occurs (Fig. 3 and 4) most notably in the experiments of longer duration (DML-1, DML-3, SIDP-1, and SIDP-2 columns), and provides compelling evidence that matrix diffusion affects the morphology of these breakthrough curves. Results are similar to those observed in a column of fractured saprolite (Moline et al., 1997). Further evidence of matrix diffusion is contained in the response to rinsing the columns, where low concentrations of solutes were detected (so-called "elongated tails") even when rinsed for twice the time of injection (Fig. 3 and 4). Mass-balance calculations indicate that 15 to 35% of the conservative solutes remained in the shallow columns after being rinsed for 1 to 2 PV. Hence, nonpoint-source contaminants could be stored in the matrix for later release into the environment.

Nitrate behaved as a conservative tracer during short-term experiments (<3 d) in the shallow columns and in a nonconservative manner during longer-term experiments for deeper columns. The nitrate BTCs from the

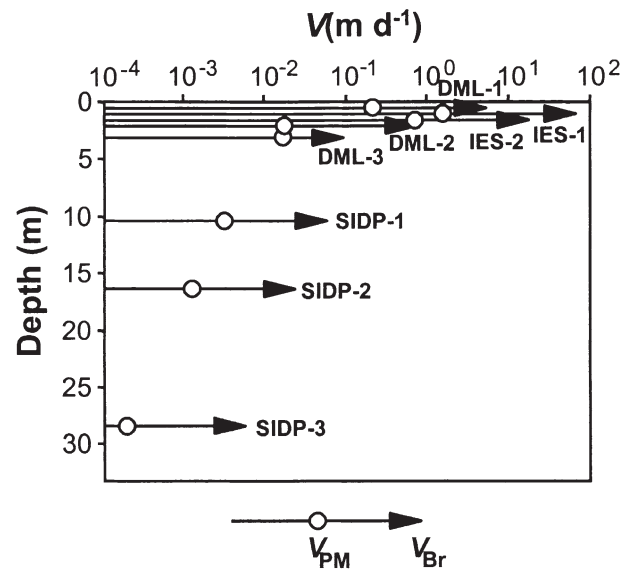


Fig. 5. Plot of velocity (log scale) versus depth for the eight till columns. Velocities are shown for time of first arrival of the bromide tracer at relative concentration (C/C_0) = 0.02 (V_{Br} , filled arrows) and for plug flow through the entire porosity of the sample calculated by Eq. [7] (V_{PM} , open circles).

DML-1, IES-1, IES-2, and DML-2 column experiments are nearly identical to the Br^- BTCs (Fig. 3). This was not the case for the DML-3 column, where the relative concentration of nitrate in the effluent remained below 0.05 for the duration of the experiment (Fig. 4). Nitrate was not detected in effluent during the SIDP-1, SIDP-2, or SIDP-3 column experiments, indicating that nitrate degraded more quickly (presumably by denitrification) in the deeper till units.

Atrazine behaved nonconservatively in all eight columns. In the experiments using the shallow columns (DML-1, IES-1, IES-2, and DML-2 columns; Fig. 3), atrazine breakthrough ($C/C_0 = 0.5$) was delayed by a factor of approximately two with respect to the conservative tracers (Br^- , PFBA, and PIPES). In addition, the maximum concentration of atrazine was about 80% of the conservative tracers during the rising limb of these BTCs. On the falling limb of the same BTCs, atrazine exceeded the concentration of the conservative tracers. This tailing phenomenon suggests that sorption, rather than degradation, is the main process acting to retard atrazine, particularly in some of the longer-term experiments (see DML-3 and SIDP-1 in Fig. 4). In the DML-3 BTC, atrazine attained an equilibrium concentration of approximately 30% of that for the conservative tracers after 30 d. Similarly, during the SIDP-1 column experiment, atrazine attained equilibrium at $C/C_0 = 0.07$ after 40 d. Atrazine was not detected in outflow during the SIDP-2 or SIDP-3 experiments, suggesting that atrazine sorption coupled with the low K_b of these deeper till units may have increased residence time sufficiently such that degradation of atrazine occurred. Effluent samples were not analyzed for atrazine degradates.

Application of the Mobile-Immobile Model

The BTCs simulated by the MIM using values of fracture porosity calculated by the Cubic Law (Eq. [5])

Table 2. Dispersion coefficient (D), mass-exchange coefficient (α), sorption coefficient (K_d), and degradation coefficient (μ) estimated by the mobile-immobile model (MIM).

Column [†]	Compound [‡]	D $\text{m}^2 \text{s}^{-1}$	α s^{-1}	K_d $\text{m}^3 \text{kg}^{-1}$	μ s^{-1}	d_1 [§]
DML-1	Br ⁻	1.9×10^{-6}	4.8×10^{-5}	NE	NE	0.91
	PFBA	1.7×10^{-6}	3.0×10^{-5}	NE	NE	0.84
	PIPES	2.5×10^{-6}	1.4×10^{-4}	NE	NE	0.94
	NO ₃ ⁻	1.9×10^{-6}	4.8×10^{-5}	NE	1.4×10^{-6}	0.92
	atrazine	1.2×10^{-6}	7.2×10^{-6}	7.2×10^{-5}	2.8×10^{-6}	0.95
DML-2	Br ⁻	1.4×10^{-5}	2.2×10^{-3}	NE	NE	0.92
	PFBA	1.5×10^{-5}	4.8×10^{-3}	NE	NE	0.92
	PIPES	1.6×10^{-5}	4.1×10^{-3}	NE	NE	0.92
	NO ₃ ⁻	1.3×10^{-5}	4.8×10^{-5}	NE	5.4×10^{-7}	0.93
	atrazine	2.4×10^{-5}	1.8×10^{-3}	3.3×10^{-4}	5.1×10^{-6}	0.91
DML-3	Br ⁻	1.8×10^{-9}	1.5×10^{-6}	NE	NE	0.98
	PFBA	1.4×10^{-9}	1.2×10^{-6}	NE	NE	0.98
	PIPES	4.3×10^{-8}	1.5×10^{-5}	NE	NE	0.97
	NO ₃ ⁻	2.1×10^{-8}	4.2×10^{-5}	NE	3.4×10^{-6}	0.72
	atrazine	6.1×10^{-8}	6.5×10^{-5}	1.5×10^{-4}	4.7×10^{-7}	0.96
IES-1	Br ⁻	8.8×10^{-5}	8.5×10^{-3}	NE	NE	0.95
	PFBA	1.0×10^{-4}	9.8×10^{-3}	NE	NE	0.94
	PIPES	1.0×10^{-4}	9.8×10^{-3}	NE	NE	0.94
	NO ₃ ⁻	8.7×10^{-5}	1.7×10^{-2}	NE	3.4×10^{-5}	0.97
	atrazine	2.7×10^{-4}	4.5×10^{-5}	1.0×10^{-3}	2.7×10^{-7}	0.86
IES-2	Br ⁻	2.2×10^{-5}	2.3×10^{-3}	NE	NE	0.92
	PFBA	2.7×10^{-5}	4.1×10^{-3}	NE	NE	0.90
	PIPES	2.8×10^{-5}	9.0×10^{-3}	NE	NE	0.90
	NO ₃ ⁻	2.3×10^{-5}	2.7×10^{-3}	NE	1.2×10^{-7}	0.92
	atrazine	7.3×10^{-7}	4.2×10^{-6}	2.6×10^{-5}	2.9×10^{-8}	0.96
SIDP-1	Br ⁻	1.5×10^{-8}	4.6×10^{-6}	NE	NE	0.97
	PFBA	1.6×10^{-8}	2.7×10^{-6}	NE	NE	0.97
	PIPES	2.1×10^{-8}	1.1×10^{-5}	NE	NE	0.96
	NO ₃ ⁻	4.7×10^{-8}	5.2×10^{-6}	2.8×10^{-4}	8.4×10^{-7}	0.76
SIDP-2	Br ⁻	1.6×10^{-9}	3.5×10^{-7}	NE	NE	0.98
	PFBA	1.6×10^{-9}	2.6×10^{-7}	NE	NE	0.96
	PIPES	1.8×10^{-9}	2.2×10^{-7}	NE	NE	0.96
SIDP-3	Br ⁻	7.9×10^{-10}	1.3×10^{-7}	NE	NE	0.78
	PFBA	8.7×10^{-10}	1.0×10^{-8}	NE	NE	0.50
	PIPES	2.0×10^{-10}	2.0×10^{-8}	NE	NE	0.66

[†] DML, Des Moines Lobe; IES, Iowan Erosion Surface; SIDP, Southern Iowa Drift Plain. See Fig. 1 for locations..

[‡] PFBA, pentafluorobenzoic acid; PIPES, 1,4-piperazinediethanesulfonic acid disodium salt.

[§] The modified index of agreement (d_1) provides a goodness-of-fit statistic between the MIM and observed data.

^{||} The terms K_d and μ were not estimated (NE) for nonsorbing and nondegrading compounds, respectively, and are omitted where solutes were not detected.

and measured values of fracture spacing and hydraulic conductivity agreed closely with those generated by the column experiments (Fig. 3 and 4). The d_1 values for the measured and simulated concentrations show a median of 0.93, a minimum of 0.50, and a maximum of 0.98 (Table 2). Eighty percent of the d_1 values were 0.90 or greater, indicating that the model fit the data well. In cases where concentrations were low during the entire BTC (less than a relative concentration of 0.1), d_1 dropped below 0.8, indicating a poorer goodness-of-fit. We believe that the ability of the MIM to fit the BTCs with the specified θ_f provides additional evidence of macropore- or fracture-controlled solute transport through the columns. It would be relatively straightforward to implement the MIM at the field scale and for long time periods due to its computational efficiency (simulations required less than a few seconds to run) and relative ease of determining input parameters (e.g., explicit fracture geometry is not required for this model). However, further study is required (possibly field-scale tracer tests) to investigate whether the parameters determined in this study remain accurate at larger spatial or temporal scales.

The MIM simulations confirm that matrix diffusion is an important process for controlling solute transport. Values of α were greater than zero (indicating matrix diffusion) and spanned six orders of magnitude, from 1×10^{-8} to $1.7 \times 10^{-2} \text{ s}^{-1}$ (Table 2). To model these

systems without matrix diffusion (α set to zero) would be inappropriate and would result in much poorer fits. These values of α should be considered approximate, however, because they were determined by the inverse method, which has been shown to produce nonunique and/or insensitive estimates of α (Parker and van Genuchten, 1984). Independent estimates of α for Br⁻, PFBA, and PIPES determined by the radial diffusion method in these tills (Helmke et al., 2004) resulted in values that were one to two orders of magnitude less than those estimated by fitting the MIM to BTCs. In addition, not all of the MIM-estimated values of α increase as a function of D_0 (i.e., PIPES should have the smallest α , followed by PFBA, then Br⁻), which indicates that the accuracy of using the inverse method is suspect. We therefore conclude that these MIM estimates of α serve as a qualitative measure of the importance of matrix diffusion, and should not be considered precise measures of diffusion rates.

Estimates of K_d from the MIM, which ranged from 2.6×10^{-5} to $1 \times 10^{-3} \text{ m}^3 \text{ kg}^{-1}$ (Table 2), also indicate that sorption retards atrazine in these till units. Sorption of atrazine was determined for the same till units at similar depths using batch-equilibrium experiments (Moorman et al., 2001). Sorption coefficients of atrazine in that study ranged from 3.1×10^{-4} to $2 \times 10^{-3} \text{ m}^3 \text{ kg}^{-1}$ using the Freundlich isotherm. Independent estimates of K_d were

similar (within a factor of 10) to those estimated by the MIM. Values of R calculated from estimated K_d values ranged from 1.2 to 6.8, which demonstrates that sorption serves to retard atrazine in addition to matrix diffusion in these tills.

Degradation appears rapid enough to cause measurable loss of both atrazine and nitrate during transport, based on MIM-estimated values of the degradation coefficient (μ). Estimates of μ ranged from 1.2×10^{-7} to $3.4 \times 10^{-5} \text{ s}^{-1}$ for nitrate and 2.9×10^{-8} to $5.1 \times 10^{-6} \text{ s}^{-1}$ for atrazine (Table 2), equating to half-lives between 0.24 and 67 d for nitrate and 1.6 and 277 d for atrazine. Cambardella et al. (1999) suggested a nitrate half-life of approximately 225 d in unoxidized (unweathered) till in central Iowa. First-order degradation coefficients have not been independently determined for atrazine in till in Iowa. However, estimated half-lives of atrazine degradation in this study are similar to those reported in the literature (20–200 d; Jury et al., 1987). At these degradation rates, it is unlikely that nitrate or atrazine could persist in the deeper, unweathered till units for more than a few months or years. This may be due to the increase in organic carbon in this material and the onset of denitrification in the matrix (Simpkins and Parkin, 1993; Parkin and Simpkins, 1995). However, the rapid velocities observed in the shallow till units suggest that both compounds could travel unaltered laterally or vertically at rates great enough to contaminate shallow aquifers and streams.

Dye Experiment

Results of the dye experiment provide further evidence that fractures control flow and transport through the till units. Upon dissection of the DML-3 column, dye was present in approximately 60% of the iron-stained fractures (Fig. 6), and absent in areas of the matrix where there were no fractures. Because dye was absent

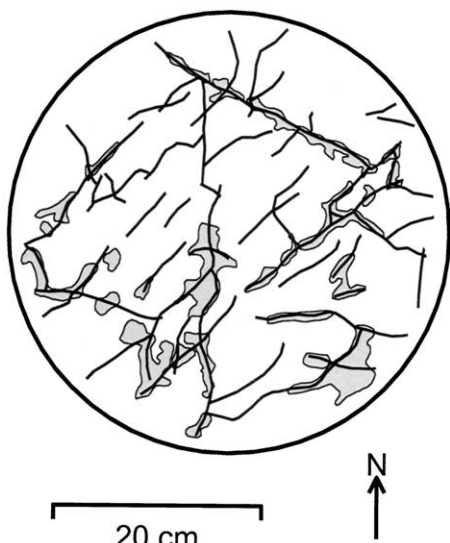


Fig. 6. Plan view of a slice taken from the center of the DML-3 column (from the Des Moines Lobe) showing fractures (dark lines) and extent of FDC Brilliant Blue Dye no. 1 (gray zones) at a depth of 3.65 m.

from some fractures, it appears that some fractures were more conductive than others. In contrast, Jørgensen et al. (1998) injected fluorescent dye into large columns of fractured till in Denmark and noted that between 80 and 100% of the fractures contained dye on dissection. Perhaps, if given enough time, the dye would have entered all fractures in our column. However, it is equally likely that, if the experiment had been allowed to progress further, the haloes surrounding each fracture would have converged and completely obscured the results of the experiment.

CONCLUSIONS

Results of this study indicate that transport of three conservative solutes (KBr, PFBA, and PIPES) and two nonconservative solutes (nitrate and atrazine) through four till units was controlled by fractures and matrix diffusion. Evidence included rapid first arrival velocities, the shape of the BTCs and success in modeling with the MIM, the separation of the rising and falling limbs of BTCs due to the different D_0 values of the tracers, the extended tails of BTCs, the inability to remove only 65 to 85% of the solutes immediately after rinsing the columns, and results of the dye experiment. Fractures were encountered in till at the three study sites and at all depths to 30.1 m. The networks were dense, with fracture spacing ranging from 3.4 to 17.8 cm. Although we sampled only three representative sites in the state and four till units, the abundance of fractures at each site and evidence of fractures elsewhere suggests that fractures and fracture flow are widespread in the till units of Iowa. Density and connectivity of the fractures appear to be more important for solute transport than orientation of the fractures or the age of the till.

The potential for fractures to transport nitrate and atrazine and affect water quality varies with depth. Nitrate was unaltered in the shallowest columns in weathered till, but showed evidence of retardation or complete degradation in columns in partially weathered and unweathered till. Fracture-controlled transport of atrazine occurs in weathered till, but due to sorption its velocity is retarded with respect to nitrate. Transport velocities in unweathered fractured till may be low enough to allow for complete degradation of atrazine before entering an aquifer or stream.

Assuming the columns are representative of the till in Iowa, our results suggest that thin, weathered till units are not likely to provide complete protection for underlying aquifers or adjacent aquifers and surface waters. Matrix diffusion may also store nonpoint-source contaminants in the till matrix for later release, providing a legacy of past contamination activities well into the future.

ACKNOWLEDGMENTS

This research was funded by grants from the American Geophysical Union (Horton Grant), the National Ground Water Association (Association of Ground Water Scientists and Engineers), the Geological Society of America and its Hydrogeology Division, Sigma Xi, USDA, and the USEPA through

Interagency Agreement DW12036252 to the Agricultural Research Service. We thank Tom Moorman, Beth Douglas, and Alistair Reungsang at the National Soil Tilth Laboratory for atrazine analyses, Phil Jardine and Geryllynn Moline for suggesting PIPES as a tracer, and Peter Jørgensen and Johnny Fredericia for advice on extracting large till columns and implementing the tracer experiments. The authors appreciate the constructive comments of Renduo Zhang and two anonymous reviewers.

REFERENCES

- Bowman, R.S., and J.S. Gibbens. 1992. Difluorobenzoates as nonreactive tracers in soil and ground water. *Ground Water* 30:8–14.
- Brockman, C.S., and J.P. Szabo. 2000. Fractures and their distribution in the tills of Ohio. *Ohio J. Sci.* 100:39–55.
- Cambardella, C.A., T.B. Moorman, D.B. Jaynes, J.L. Hatfield, T.B. Parkin, W.W. Simpkins, and D.L. Karlen. 1999. Water quality in Walnut Creek watershed: Nitrate-nitrogen in soils, subsurface drainage water, and shallow groundwater. *J. Environ. Qual.* 28:25–34.
- Coats, K.H., and B.D. Smith. 1964. Dead-end pore volume and dispersion in porous media. *Soc. Pet. Eng. J.* 4:73–84.
- Connell, D.E. 1984. Distribution, characteristics, and genesis of joints in fine-grained till and lacustrine sediments, eastern and northwestern Wisconsin. M.S. thesis. Univ. of Wisconsin, Madison.
- D'Astous, A.Y., W.W. Ruland, J.R.G. Bruce, J.A. Cherry, and R.W. Gillham. 1989. Fracture effects in the shallow groundwater zone in weathered Sarnia-area clay. *Can. Geotech. J.* 26:43–56.
- Eidem, J.M., W.W. Simpkins, and M.R. Burkart. 1999. Geology, groundwater flow, and water quality in the Walnut Creek watershed. *J. Environ. Qual.* 28:60–69.
- Flury, M., and H. Flüher. 1995. Tracer characteristics of Brilliant Blue FCF. *Soil Sci. Soc. Am. J.* 59:22–27.
- Freeze, R.A., and J.A. Cherry. 1979. *Groundwater*. Prentice Hall, New York.
- Gaber, H.M., W.P. Inskeep, S.D. Comfort, and J.M. Wraith. 1995. Nonequilibrium transport of atrazine through large intact soil cores. *Soil Sci. Soc. Am. J.* 59:60–67.
- Grisak, G.E., and J.F. Pickens. 1980. Solute transport through fractured media: 1. The effect of matrix diffusion. *Water Resour. Res.* 16:719–730.
- Grisak, G.E., J.F. Pickens, and J.A. Cherry. 1980. Solute transport through fractured media: 2. Column study of fractured till. *Water Resour. Res.* 16:731–739.
- Gwo, J.P., R. O'Brien, and P.M. Jardine. 1998. Mass transfer in structured porous media: Embedding mesoscale structure and microscale hydrodynamics in a two-region model. *J. Hydrol. (Amsterdam)* 208:204–222.
- Harris, D.C. 1991. *Quantitative chemical analysis*. 3rd ed. W.H. Freeman, New York.
- Helmke, M.F. 2003. Studies of solute transport through fractured till in Iowa. Ph.D. diss. Iowa State Univ., Ames.
- Helmke, M.F., W.W. Simpkins, and R. Horton. 2004. Experimental determination of effective diffusion parameters in the matrix of fractured till. *Vadose Zone J.* 3:1050–1056.
- Herzog, B.L., R.A. Griffin, C.J. Stohr, L.R. Follmer, W.J. Morse, and W.J. Su. 1989. Investigation of failure mechanisms and migration of organic chemicals at Wilsonville, Illinois. *Ground Water Monit. Rev.* 9:82–89.
- Jaynes, D.B. 1993. Evaluation of fluorobenzoate tracers in surface soils. *Ground Water* 32:532–538.
- Jørgensen, P.R., and J. Fredericia. 1992. Migration of nutrients, pesticides and heavy metals in fractured clayey till. *Geotechnique* 42:67–77.
- Jørgensen, P.R., L.D. McKay, and N.Z.H. Spliid. 1998. Evaluation of chloride and pesticide transport in a fractured clayey till using large undisturbed columns and numerical modeling. *Water Resour. Res.* 34:539–553.
- Jørgensen, P.R., and N.H. Spliid. 1992. Mechanisms and rates of pesticide leaching in shallow clayey till. p. 1–11. *In* European Conf. on Integrated Res. for Soil and Sediment Protection and Remediation, Maastricht, the Netherlands. 6–12 Sept. 1992. Kluwer Academic Publ., Dordrecht, the Netherlands.
- Jury, W.A., D.D. Focht, and W.J. Farmer. 1987. Evaluation of pesticide groundwater pollution potential from standard indices of soil-chemical adsorption and biodegradation. *J. Environ. Qual.* 16:422–428.
- Keller, C.K., G. van der Kamp, and J.A. Cherry. 1988. Hydrogeology of two Saskatchewan tills. I. Fractures, bulk permeability, and special variability of downward flow. *J. Hydrol. (Amsterdam)* 101:97–121.
- Keller, C.K., G. van der Kamp, and J.A. Cherry. 1989. A multiscale study of the permeability of a thick clayey till. *Water Resour. Res.* 25:2299–2317.
- Kemmis, T.J., E.A. Bettis III, and G.R. Hallberg. 1992. Quaternary geology of Conklin Quarry. Guidebook Ser. no. 13. Iowa Dep. of Natural Resour., Des Moines.
- Kemmis, T.J., G.R. Hallberg, and A.J. Lutenecker. 1981. Depositional environments of glacial sediments and landforms on the Des Moines Lobe, Iowa. Guidebook Ser. 6. Iowa Dep. of Natural Resour., Des Moines.
- Klint, K.E.S., and P. Gravensten. 1999. Fractures and biopores in Weichselian clayey till aquitards at Flakkebjerg, Denmark. *Nord. Hydrol.* 30:267–284.
- Kluitenberg, G.L., J.R. Bilskie, and R. Horton. 1991. Rubberized asphalt for sealing cores of shrinking soil. *Soil Sci. Soc. Am. J.* 55:1504–1507.
- Kolpin, D.W., E.M. Thurman, and S.M. Linhart. 2000. Finding minimal herbicide concentrations in ground water? Try looking for their degradates. *Sci. Total Environ.* 248:115–122.
- Kross, B.C., G.R. Hallberg, D.R. Bruner, R.D. Libra, K.D. Rex, L.M.B. Weih, M.E. Vermace, L.F. Burmeister, N.H. Hall, K.L. Cherrylomes, J.K. Johnson, M.I. Selim, B.K. Nations, L.S. Seigley, D.J. Quaide, A.G. Dudler, K.D. Sesker, M.A. Culp, C.F. Lynch, H.F. Nicholson, and J. Hughes. 1990. The Iowa State-Wide Rural Well-Water Survey, water quality data: Initial analysis. Tech. Info. Ser. 19. Iowa Dep. of Natural Resour., Des Moines.
- Legates, D.R., and G.J. McCabe, Jr. 1999. Evaluating the use of “goodness-of-fit” measures in hydrologic and hydroclimatic model validation. *Water Resour. Res.* 35:233–241.
- Marquardt, D.W. 1963. An algorithm for least-squares estimation of nonlinear parameters. *J. Soc. Ind. Appl. Math.* 11:431–441.
- Mayes, M.A., P.M. Jardine, T.L. Mehlhorn, B.N. Bjornstad, J.L. Ladd, and J.M. Zachara. 2003. Transport of multiple tracers in variably saturated humid region structured soils and semi-arid region laminated sediments. *J. Hydrol. (Amsterdam)* 275:141–161.
- McKay, L.D., D.J. Balfour, and J.A. Cherry. 1998. Lateral chloride migration from a landfill in a fractured clay-rich glacial deposit. *Ground Water* 36:988–999.
- McKay, L.D., J.A. Cherry, and R.W. Gillham. 1993a. Field experiments in a fractured clay till: 1. Hydraulic conductivity and fracture aperture. *Water Resour. Res.* 29:1149–1162.
- McKay, L.D., J.A. Cherry, and R.W. Gillham. 1993b. Field experiments in a fractured clay till: 2. Solute and colloid transport. *Water Resour. Res.* 29:3879–3890.
- McKay, L.D., and J. Fredericia. 1995. Distribution, origin, and hydraulic influence of fractures in a clay-rich glacial deposit. *Can. Geotech. J.* 32:957–975.
- Moline, G.R., C.R. Knight, and R. Ketcham. 1997. Laboratory measurement of transport processes in a fractured limestone/shale saprolite using solute and colloid tracers. *Geol. Soc. Am. Abstr. Programs* 29:370.
- Moorman, T.B., K. Jayachandran, and A. Reungsang. 2001. Adsorption and desorption of atrazine in soils and subsurface sediments. *Soil Sci.* 166:921–929.
- Moorman, T.B., D.B. Jaynes, C.A. Cambardella, J.L. Hatfield, R.L. Pfeiffer, and A.J. Morrow. 1999. Water quality in Walnut Creek watershed: Herbicides in soils, subsurface drainage, and groundwater. *J. Environ. Qual.* 28:35–45.
- National Research Council. 1929. *International critical tables of numerical data, physics, chemistry and technology*. Version 5. McGraw-Hill, New York.
- Parker, J.C., and M.Th. van Genuchten. 1984. Determining transport parameters from laboratory and field tracer experiments. *Virginia Agric. Exp. Stn. Bull.* 84. Virginia Polytechnic and State Univ., Blacksburg.
- Parkin, T.B., and W.W. Simpkins. 1995. Contemporary groundwater

- methane production from Pleistocene carbon. *J. Environ. Qual.* 24: 367-372.
- Prior, J.C. 1991. Landforms of Iowa. Univ. of Iowa Press, Iowa City.
- Rodvang, S.J., and W.W. Simpkins. 2001. Agricultural contaminants in Quaternary aquitards: A review of occurrence and fate in North America. *Hydrogeol. J.* 9:44-59.
- Scott, H.D., and R.E. Phillips. 1973. Self-diffusion coefficients of selected herbicides in water and estimates of their transmission factors in soil. *Soil Sci. Soc. Am. Proc.* 37:965-967.
- Seo, H.H. 1996. Hydraulic properties of Quaternary stratigraphic units in the Walnut Creek watershed. M.S. thesis. Iowa State Univ., Ames.
- Seo, H.H., J.M. Eidem, and W.W. Simpkins. 1996. Hydraulic properties of Quaternary units in the Walnut Creek watershed. p. 59-67. *In* Hydrogeology and water quality of the Walnut Creek watershed. Geol. Survey Bureau Guidebook Ser. 20. Iowa Dep. of Natural Resour., Des Moines.
- Simpkins, W.W., and K.R. Bradbury. 1992. Groundwater flow, velocity, and age in a thick, fine-grained till unit in southeastern Wisconsin. *J. Hydrol. (Amsterdam)* 132:283-319.
- Simpkins, W.W., M.R. Burkart, M.F. Helmke, T.N. Twedt, D.E. James, R.J. Jaquis, and K.J. Cole. 2002. Potential impact of earthen waste storage structures on water resources in Iowa. *J. Am. Water Resour. Assoc.* 38:759-771.
- Simpkins, W.W., and T.B. Parkin. 1993. Hydrogeology and redox geochemistry of methane in a late Wisconsinan till and loess sequence in central Iowa. *Water Resour. Res.* 29:3643-3657.
- Snow, D.T. 1969. Anisotropic permeability of fractured media. *Water Resour. Res.* 5:1273-1289.
- Sudicky, E.A. 1990. The Laplace transform Galerkin technique for efficient time-continuous solution of solute transport in double-porosity media. *Geoderma* 46:209-232.
- Toride, N., F.J. Leij, and M.Th. van Genuchten. 1999. The CXTFIT code for estimating transport parameters from laboratory or field tracer experiments. Res. Rep. 137. U.S. Salinity Lab., USDA-ARS, Riverside, CA.
- Van Genuchten, M.Th. 1981. Non-equilibrium transport parameters from miscible displacement experiments. Res. Rep. 119. U.S. Salinity Lab., USDA-ARS, Riverside, CA.
- Van Genuchten, M.Th., and R.J. Wagenet. 1989. Two-site/two-region models for pesticide transport and degradation: Theoretical development and analytical solutions. *Soil Sci. Soc. Am. J.* 53:1303-1310.
- Van Genuchten, M.Th., and P.J. Wierenga. 1976. Mass transfer studies in sorbing porous media: I. Analytical solutions. *Soil Sci. Soc. Am. J.* 40:473-481.
- Walter, N.F., G.R. Hallberg, and T.E. Fenton. 1978. Particle-size analysis by the Iowa State University Soil Survey Laboratory. p. 61-74. *In* G.R. Hallberg (ed.) Standard procedures for evaluation of Quaternary materials in Iowa. Iowa Geol. Survey Tech. Info. Ser. 8. Iowa Dep. of Natural Resour., Des Moines.
- Weis, M.R., and W.W. Simpkins. 1996. Nitrate and herbicide transport in groundwater within fractured, Pre-Illinoian till units near Nashua, Iowa. *Geol. Soc. Am. Abstr. Programs* 28:70.
- Willmott, C.J., S.G. Ackleson, R.E. Davis, J.J. Feddema, K.M. Klink, D.R. Legates, J. O'Donnell, and C.M. Rowe. 1985. Statistics for the evaluation and comparison of models. *J. Geophys. Res. [Oceans]* 90:8995-9005.